Progress In Electromagnetics Research, PIER 92, 91–102, 2009

DIRECTIVE EM RADIATION OF A LINE SOURCE IN THE PRESENCE OF A COATED PEMC CIRCULAR CYLINDER

S. Ahmed and Q. A. Naqvi

Department of Electronics
Quaid-i-Azam University
Islamabad, Pakistan

Abstract—Electromagnetic scattering of a line source from a perfect electromagnetic conductor (PEMC) circular cylinder coated with double positive (DPS) material or double negative (DNG) material is investigated theoretically. The response of the coated PEMC circular cylinder is observed and it is noted that how the results obtained for this configuration differ from those of a coated perfect electric conductor (PEC) circular cylinder. It is assumed that both the PEMC cylinder and the coating layer are infinite along the cylinder axis. The comparison of directivity of coated PEMC cylinder and coated PEC cylinder is presented.

1. INTRODUCTION

Perfect electromagnetic conductor (PEMC) medium introduced by Lindell and Sihvila [1] displays truly special properties. It is a very fundamental type of medium and many researchers have worked on this material [1–16]. The PEMC medium is defined by the following constitutive relations in between the electric field $\mathbf{E}$ and magnetic field $\mathbf{H}$ fields and electric displacement $\mathbf{D}$ and magnetic displacement $\mathbf{B}$ as given below

$$\mathbf{D} = M\mathbf{B}, \qquad \mathbf{H} = -M\mathbf{E} \tag{1}$$

where M is a real scalar admittance parameter. The normal component of the Poynting vector at the PEMC boundary vanishes, that is

$$\begin{aligned} \mathbf{n} \cdot (\mathbf{E} \times \mathbf{H}) &= -\mathbf{E} \cdot (\mathbf{n} \times \mathbf{H}) \\ &= M\mathbf{E} \cdot (\mathbf{n} \times \mathbf{E}) = 0 \end{aligned} \tag{2}$$

Corresponding author: Q. A. Naqvi (qaisar@qau.edu.pk).

This means that PEMC medium serves as an ideal boundary. The PMC and PEC boundary conditions are the two limits of the PEMC boundary condtions

$$M \to 0\,(\text{PMC}): \quad \mathbf{n} \times \mathbf{H} = 0, \quad \mathbf{n} \cdot \mathbf{D} = 0 \tag{3}$$

$$M \to \pm\infty\,(\text{PEC}): \quad \mathbf{n} \times \mathbf{E} = 0, \quad \mathbf{n} \cdot \mathbf{B} = 0 \tag{4}$$

Electromagnetic scattering by coated circular cylinders is a classical problem in electromagnetics and has been investigated by several researchers [17–28]. Scattering behavior becomes much more complicated if scattering obstacle is made of layers or sections of several materials. This is because of presence of unavoidable multiple scattering at the boundary surfaces, i.e., multiple reflection, refraction and interference. Tang [17, 18], found the theoretical and experimental results for the backscattering from coated cylinders where the thickness of the dielectric coating was comparable to the wavelength. Wang [19] converted the eigenfunction solution into a high frequency ray solution and expressed the scattered fields in terms of geometrical ray and two surface waves around the cylinder. Scattering of electromagnetic waves by an anisotropic plasma-coated conducting cylinder was considered by Chen and Cheng [20]. Electromagnetic scattering by an impedance cylinder coated eccentrically with a chiroplasma cylinder was discussed by Shen [21]. Shen and Li [22], studied electromagnetic scattering by a conducting cylinder coated with metamaterials. The scattered TM fields for two plane waves incident on a circular cylinder covered by a dielectric material, were investigated by Mushref [23]. A closed series solution of electromagnetic scattering by an eccentric coated cylinder in matrix form was achieved by Mushref [24]. While Sun et al. [25], analyzed the electromagnetic radiation of a line source scattered by an infinite conducting cylinder coated left-handed metamaterial(LHM). Irci and Ertürk [27] used the metamaterial coated conducting cylinder to achieve transparency and scattering maximization. In this paper, we have studied the response of a coated PEMC circular cylinder to the line source radiation.

2. FORMULATION

The geometry of the scattering problem is shown in Fig. 1, where the inner cylinder is a PEMC cylinder while the outer cylinder is the metamaterial coating of uniform thickness. The radius of the inner cylinder is a and the radius of the coating cylinder is b. A line source located at (ρ_0, ϕ_0), is used as the source of excitation for the configuration. The cylinders are supposed to be infinite along their axes and circular cross section. Two cases have been discussed in the

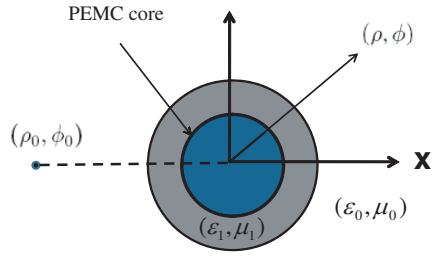

Figure 1. Geometry of the problem.

first case line source is placed outside the coating layer and in the second case the line source is placed inside the coating layer.

For the case of the line source outside the coating layer, the geometry has been divided into three regions. The region occupying the space away from the line source, i.e., $\rho \geq \rho_0$ is named as Region I. And the region between the line source and the coating layer, i.e., $b \leq \rho \leq \rho_0$ is named as Region II. Region I and Region II are free space with (μ_0, ϵ_0), and wavenumber $k_0 = \omega\sqrt{\mu_0\epsilon_0}$. While metamaterial layer $a \leq \rho \leq b$, with $k_1 = \omega\sqrt{\mu_1\epsilon_1}$ is taken as Region III. The incident electric field from the line source is given by

$$E_{0z}^{\text{inc}}(\rho,\, \phi) = -\frac{k_0^2 I}{4\omega\epsilon_0} H_n^{(1)}(k_0|\boldsymbol{\rho} - \boldsymbol{\rho}_0|) \tag{5}$$

Using addition theorem of Hankel functions, above can be written as

$$E_z^{\text{inc}}(\rho,\phi) = \begin{cases} -\dfrac{k_0^2 I}{4\omega\varepsilon_0} \displaystyle\sum_{n=-\infty}^{\infty} H_n^{(1)}(k_0\rho_0) J_n(k_0\rho) e^{jn(\phi-\phi_0)} & b \leq \rho \leq \rho_0 \\ -\dfrac{k_0^2 I}{4\omega\varepsilon_0} \displaystyle\sum_{n=-\infty}^{\infty} J_n(k_0\rho_0) H_n^{(1)}(k_0\rho) e^{jn(\phi-\phi_0)} & \rho_0 \leq \rho \end{cases} \tag{6}$$

As the core is a PEMC circular cylinder, the scattered field will contain a cross-polarized field component in addition to the co-polarized field component. The total fields in Region I, in terms of unknown expansion coefficients are given by following expressions

$$E_z^{\text{I}} = -\frac{k_0^2 I}{4\omega\epsilon_0} \sum_{n=-\infty}^{\infty} H_n^{(1)}(k_0\rho)\Big[J_n(k_0\rho_0) + a_n H_n^{(1)}(k_0\rho_0)\Big] e^{jn(\phi-\phi_0)} \tag{7}$$

$$H_\phi^{\text{I}} = \frac{k_0^2 I}{4j\omega\epsilon_0\eta_0} \sum_{n=-\infty}^{\infty} H_n^{(1)\prime}(k_0\rho)\Big[J_n(k_0\rho_0) + a_n H_n^{(1)}(k_0\rho_0)\Big] e^{jn(\phi-\phi_0)} \tag{8}$$

$$H_z^{\mathrm{I}} = -\frac{k_0^2 I}{4j\omega\epsilon_0\eta_0}\sum_{n=-\infty}^{\infty} H_n^{(1)}(k_0\rho)\Big[J_n(k_0\rho_0)+b_n H_n^{(1)}(k_0\rho_0)\Big]e^{jn(\phi-\phi_0)} \quad (9)$$

$$E_\phi^{\mathrm{I}} = \frac{k_0^2 I}{4\omega\epsilon_0}\sum_{n=-\infty}^{\infty} H_n^{(1)\prime}(k_0\rho)\Big[J_n(k_0\rho_0)+b_n H_n^{(1)}(k_0\rho_0)\Big]e^{jn(\phi-\phi_0)} \quad (10)$$

where η_0 is the free space impedance and prime denotes the derivative wit respect to entire argument. While the total fields in the Region II, may be written as

$$E_z^{\mathrm{II}} = -\frac{k_0^2 I}{4\omega\epsilon_0}\sum_{n=-\infty}^{\infty} H_n^{(1)}(k_0\rho_0)\Big[J_n(k_0\rho)+a_n H_n^{(1)}(k_0\rho)\Big]e^{jn(\phi-\phi_0)} \quad (11)$$

$$H_\phi^{\mathrm{II}} = \frac{k_0^2 I}{4j\omega\epsilon_0\eta_0}\sum_{n=-\infty}^{\infty} H_n^{(1)}(k_0\rho_0)\Big[J_n'(k_0\rho)+a_n H_n^{(1)\prime}(k_0\rho)\Big]e^{jn(\phi-\phi_0)} \quad (12)$$

$$H_z^{\mathrm{II}} = -\frac{k_0^2 I}{4j\omega\epsilon_0\eta_0}\sum_{n=-\infty}^{\infty} H_n^{(1)}(k_0\rho_0)\Big[J_n(k_0\rho)+b_n H_n^{(1)}(k_0\rho)\Big]e^{jn(\phi-\phi_0)} \quad (13)$$

$$E_\phi^{\mathrm{II}} = \frac{k_0^2 I}{4\omega\epsilon_0}\sum_{n=-\infty}^{\infty} H_n^{(1)}(k_0\rho_0)\Big[J_n'(k_0\rho)+b_n H_n^{(1)\prime}(k_0\rho)\Big]e^{jn(\phi-\phi_0)} \quad (14)$$

The total fields in Region III is

$$E_z^{\mathrm{III}} = -\frac{k_0^2 I}{4\omega\epsilon_0}\sum_{n=-\infty}^{\infty} H_n^{(1)}(k_0\rho_0)\Big[c_n J_n(k_1\rho)+d_n H_n^{(1)}(k_1\rho)\Big]e^{jn(\phi-\phi_0)} \quad (15)$$

$$H_\phi^{\mathrm{III}} = \frac{k_0^2 I}{4j\omega\epsilon_0\eta_1}\sum_{n=-\infty}^{\infty} H_n^{(1)}(k_0\rho_0)\Big[c_n J_n'(k_1\rho)+d_n H_n^{(1)\prime}(k_1\rho)\Big]e^{jn(\phi-\phi_0)} \quad (16)$$

$$H_z^{\mathrm{III}} = -\frac{k_0^2 I}{4j\omega\epsilon_0\eta_1}\sum_{n=-\infty}^{\infty} H_n^{(1)}(k_0\rho_0)\Big[e_n J_n(k_1\rho)+f_n H_n^{(1)}(k_1\rho)\Big]e^{jn(\phi-\phi_0)} \quad (17)$$

$$E_\phi^{\mathrm{III}} = \frac{k_0^2 I}{4\omega\epsilon_0}\sum_{n=-\infty}^{\infty} H_n^{(1)}(k_0\rho_0)\Big[e_n J_n'(k_1\rho)+f_n H_n^{(1)\prime}(k_1\rho)\Big]e^{jn(\phi-\phi_0)} \quad (18)$$

η_1 is the impedance of the coating layer. In the above expressions a_n, b_n, c_n, d_n, e_n, and f_n are the six unknown scattering coefficients in case of the TM incident plane wave which are to be determined. These unknowns can be found by using appropriate boundary conditions at the interfaces $\rho = a$ and $\rho = b$. The boundary conditions at the

interface $\rho = a$ are

$$H_z^{\mathrm{III}} + ME_z^{\mathrm{III}} = 0, \qquad \rho = a, \qquad 0 \le \phi \le 2\pi \tag{19}$$

$$H_\phi^{\mathrm{III}} + ME_\phi^{\mathrm{III}} = 0, \qquad \rho = a, \qquad 0 \le \phi \le 2\pi \tag{20}$$

And the boundary conditions at the interface $\rho = b$ are

$$E_z^{\mathrm{II}} = E_z^{\mathrm{III}}, \qquad \rho = b, \qquad 0 \le \phi \le 2\pi \tag{21}$$

$$H_\phi^{\mathrm{II}} = H_\phi^{\mathrm{III}}, \qquad \rho = b, \qquad 0 \le \phi \le 2\pi \tag{22}$$

$$H_z^{\mathrm{II}} = H_z^{\mathrm{III}}, \qquad \rho = b, \qquad 0 \le \phi \le 2\pi \tag{23}$$

$$E_\phi^{\mathrm{II}} = E_\phi^{\mathrm{III}}, \qquad \rho = b, \qquad 0 \le \phi \le 2\pi \tag{24}$$

Application of these boundary conditions at $\rho = a$ and $\rho = b$, yields a linear matrix equation about the unknown scattering coefficients. Solution of this matrix equation gives us the values of all the unknowns scattering coefficients in the above equations. We have used the numerical technique to solve the boundary conditions for unknown scattering coefficients. That is why we have not given expression for the unknown coefficients. Using the values of a_n and b_n in Equations (7) and (10), we get the scattered co- and cross-polarized fields radiated by the coated PEMC cylinder respectively. Far-zone scattered fields are obtained by using the asymptotic form of Hankel functions. For the line source placed inside the coating layer the analysis is done on the same pattern and we have presented only the numerical results for that case.

3. SIMULATIONS

In this section, we have presented the numerical results for co- and cross-polarized of a PEMC circular cylinder coated with DPS or DNG materials. In order to verify the analytical formulation and the numerical code, the results obtained are compared with the published literature [25] and are found to be in good agreement with them. In all the plots the radius of the PEMC cylinder is taken as $a = 1.25\lambda_0$ and λ_0 is the wavelength of the free space. Also in all the plots, the full line shows the scattering behavior for PEC as special case of PEMC i.e., when $M\eta_1 \to \pm\infty$. While dashed and short dashed lines are used for co- and cross-polarized components of PEMC case with $M\eta_1 = \pm 1$, respectively. Fig. 2 presents the scattering behavior of the PEMC cylinder coated with either an ordinary dielectric DPS or a DNG, when the line source is outside the coating layer. The parameters for the scattering phenomena for this figure are, $b = 2.2\lambda_0$, $\rho_0 = 2.3\lambda_0$.

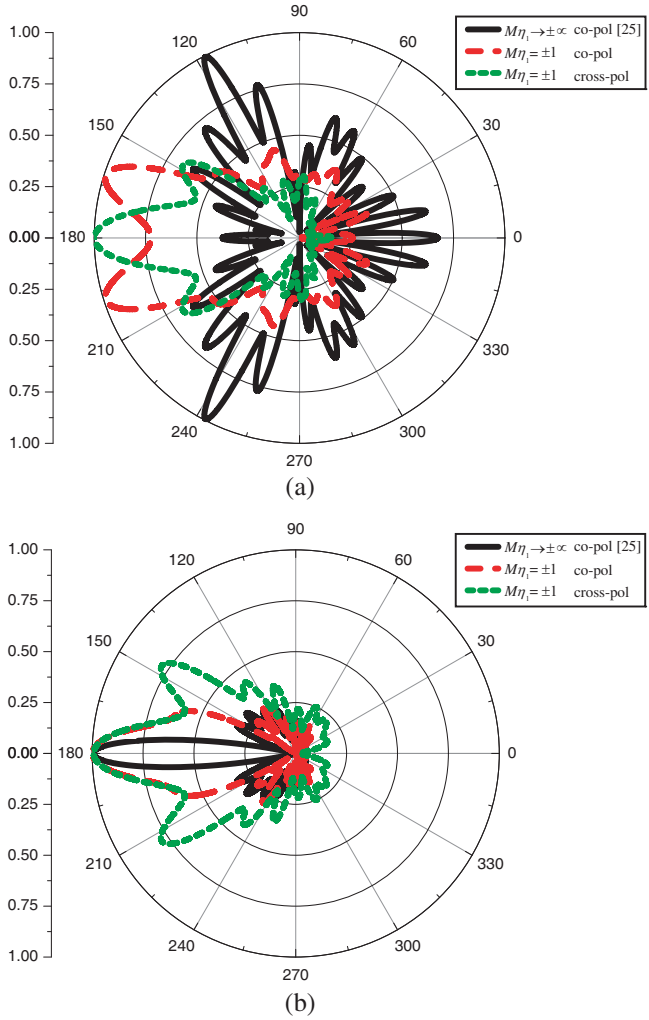

Figure 2. (a) Far-field radiation patterns of a PEMC circular cylinder coated by DPS layer ($\varepsilon_r = 1.5$, $\mu_r = 1.5$) when $a = 1.25\lambda_0$, $b = 2.2\lambda_0$, $\rho_0 = 2.3\lambda_0$, (b) far-field radiation patterns of a PEMC circular cylinder coated by DNG layer ($\varepsilon_r = -1.5$, $\mu_r = -1.5$) when $a = 1.25\lambda_0$, $b = 2.2\lambda_0$, $\rho_0 = 2.3\lambda_0$.

In Fig. 2(a), the far-field radiation patterns of a DPS coated PEMC cylinder for $\epsilon_r = 1.5$ and $\mu_r = 1.5$ are shown. From this figure, it is obvious that for an ordinary dielectric, coated PEMC cylinder is some what more directive as compared to a dielectric coated PEC

cylinder. Fig. 2(b) shows the behavior of the co- and cross-polarized components of the far-field radiation patterns of DNG coated PEMC cylinder for the same parameters as for Fig. 2(a). This figure shows that the radiation patterns due to a DNG coated PEMC cylinder are less directive than those of a PEC cylinder coated by DNG material.

Figures 3–5 are reserved for discussion about the scattering patterns of a coated PEMC cylinder when the line source is inside the coating layer. Fig. 3 gives the far-field radiation patters of the coated PEMC cylinder two types of the coating layers with $b = 3\lambda_0$,

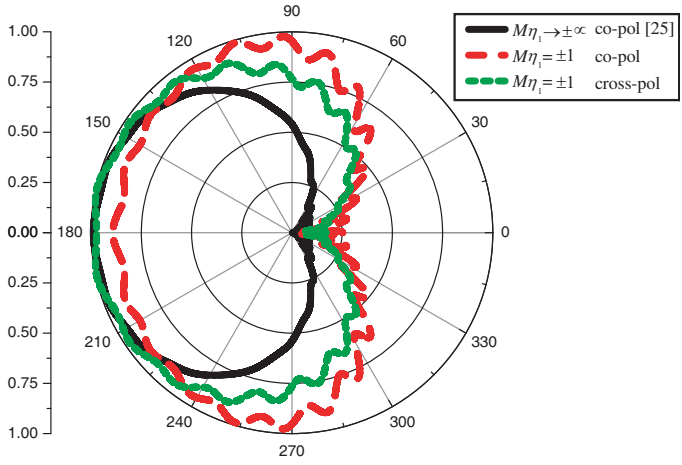

(a)

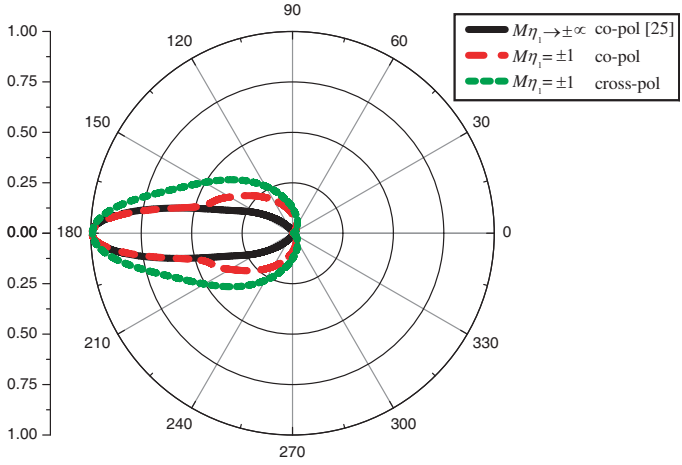

(b)

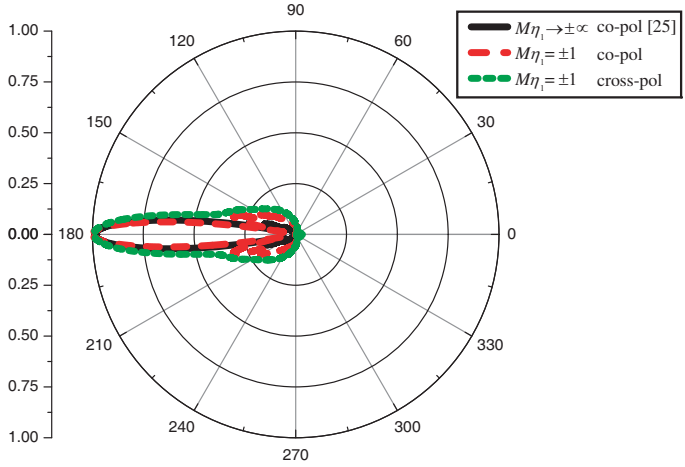

(c)

Figure 3. (a) Far-field radiation patterns of a PEMC circular cylinder coated by DPS layer ($\varepsilon_r = 1.5$, $\mu_r = 1.5$) when $a = 1.25\lambda_0$, $b = 3\lambda_0$, $\rho_0 = 1.4\lambda_0$, (b) far-field radiation patterns of a PEMC circular cylinder coated by DNG layer ($\varepsilon_r = -1$, $\mu_r = -1$) when $a = 1.25\lambda_0$, $b = 3\lambda_0$, $\rho_0 = 1.4\lambda_0$, (c) far-field radiation patterns of a PEMC circular cylinder coated by DNG layer ($\varepsilon_r = -1.5$, $\mu_r = -1.5$) when $a = 1.25\lambda_0$, $b = 3\lambda_0$, $\rho_0 = 1.4\lambda_0$.

$\rho_0 = 1.4\lambda_0$. In Fig. 3(a), the radiation patterns are shown when the coating layer is a DPS material with $\epsilon_r = 1.5$ and $\mu_r = 1.5$. This plot also predicts the difference between PEC and PEMC materials when they are used as the core of the geometry. Fig. 3(b) shows the difference between radiation patterns of a coated PEMC cylinders when it is coated by DNG metamaterial with $\epsilon_r = -1$ and $\mu_r = -1$. While Fig. 3(c) shows the far-field radiation patterns when $\epsilon_r = -1.5$ and $\mu_r = -1.5$ are taken.

Figure 4 presents the far-field radiation power gain as a function of the distance of the line source from the boundary of the core cylinder. In this figure, a DNG coating layer with $\epsilon_r = -1.5$ and $\mu_r = -1.5$, is used and the the thickness of the coating layer is taken as $b = 3\lambda_0$. It is observed from this figure that inside a PEMC circular cylinder image source of an electric line source does not exist. And as we take the line source away from the boundary of the PEMC cylinder inside the coating layer, co-polarized component of the radiation power gain increases while the cross-polarized component decreases at the same time.

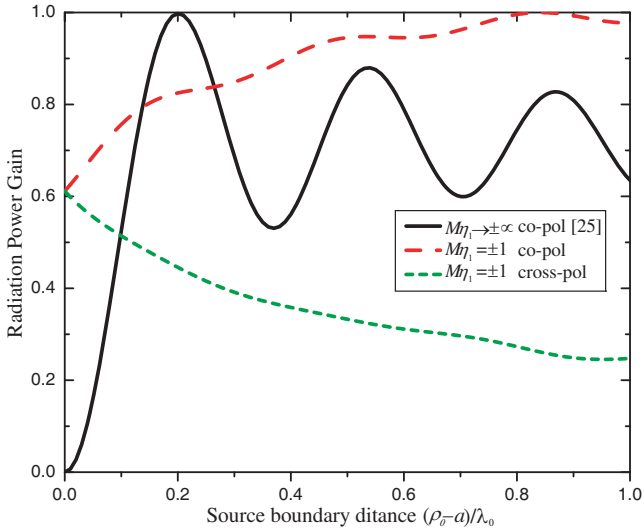

Figure 4. Radiation power gain of a PEMC circular cylinder as a function of distance of line source from the cylinder boundary when DNG coating layer is used i.e., ($\varepsilon_r = -1.5$, $\mu_r = -1.5$) when $a = 1.25\lambda_0$, $b = 3\lambda_0$, $\rho_0 = 1.4\lambda_0$.

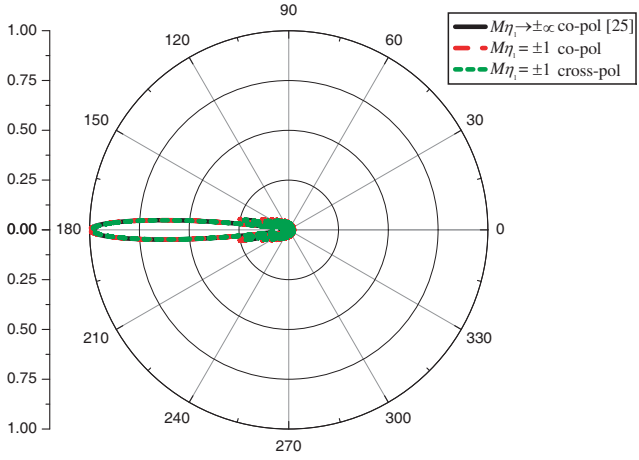

Figure 5. Far-field radiation patterns of a coated PEMC circular cylinder when dispersive DNG coating layer is used when $a = 1.25\lambda_0$, $b = 4.8\lambda_0$, $\rho_0 = 1.31\lambda_0$.

Figure 5 shows the far-field radiation patterns of a PEMC cylinder, when it is coated by a dispersive DNG layer. The DNG is taken to be lossless and the dispersion relations are taken as [25, 26]

$$\epsilon_r = 1 - \frac{\omega_p^2}{\omega^2}, \qquad \mu_r = 1 - \frac{F\omega_p^2}{\omega^2 - \omega_0^2}$$

where $\omega_0/2\pi = 4\,\text{GHz}$, $\omega_p/2\pi = 10\,\text{GHz}$, and $F = 0.56$. The frequency used in this figure is 4.35 GHz and it is seen from this figure that the directivity of the coated PEMC cylinder is the same in case of both the components as that of a coated PEC cylinder at an optimized frequency.

4. CONCLUSION

It is observed from the numerical results that in comparison to a coated PEC cylinder, the coated PEMC cylinder is some what more directive for DPS coating and is less directive for non-dispersive DNG coating when the line source is placed outside the coating layer. Also we have noted that the co-polarized component of the PEMC coated cylinder is more directive for non-dispersive DNG coating when the line source is located inside the coating layer. But this geometry is equally directive for a dispersive DNG coating, as compared to a coated PEC cylinder for the same coating as compared to a coated PEC cylinder, when line souce lies inside the coating layer.

REFERENCES

1. Lindell, I. V. and A. H. Sihvola, "Perfect electromagnetic conductor," *Journal of Electromagnetic Waves and Applications*, Vol. 19, 861–869, 2005.
2. Lindell, I. V., *Differential Forms in Electromagnetics*, Wiley and IEEE Press, New York, 2004.
3. Lindell, I. V. and A. H. Sihvola, "Realization of the PEMC boundary," *IEEE Trans. Antennas Propag.*, Vol. 53, No. 9, 3012–3018, 2005.
4. Lindell, I. V., and A. H. Sihvola, "Transformation method for problems involving perfect electromagnetic conductor (PEMC) structures," *IEEE Trans. Antennas Propag.*, Vol. 53, No. 9, 3005–3011, 2005.
5. Ruppin, R., "Scattering of electromagnetic radiation by a perfect electromagnetic conductor cylinder," *Journal of Electromagnetic Waves and Applications*, Vol. 20, No. 13, 1853–1860, 2006.

6. Lindell, I. V. and A. H. Sihvola, "Losses in PEMC boundary," *IEEE Trans. Antennas Propag.*, Vol. 54, No. 9, 2553–2558, 2006.
7. Jancewicz, B., "Plane electromagnetic wave in PEMC," *Journal of Electromagnetic Waves and Applications*, Vol. 20, No. 5, 647–659, 2006.
8. Ahmed, S. and Q. A. Naqvi, "Electromagnetic scattering from a perfect electromagnetic conductor cylinder buried in a dielectric half space," *Progress In Electromagnetics Research*, PIER 78, 25–38, 2008.
9. Ahmed, S. and Q. A. Naqvi, "Electromagnetic scattering form parallel perfect electromagnetic conductor cylinders of circular cross-sections using iterative procedure," *Journal of Electromagnetic Waves and Applications*, Vol. 22, 987–1003, 2008.
10. Ahmed, S. and Q. A. Naqvi, "Electromagnetic scattering from a two dimensional perfect electromagnetic conductor (PEMC) strip and PEMC strip grating simulated by circular cylinders," *Opt. Commun.*, Vol. 281, 4211–4218, 2008.
11. Ahmed, S. and Q. A. Naqvi, "Electromagnetic scattering from a perfect electromagnetic conductor cylinder coated with a metamaterial having negative permittivity and/or permeability," *Opt. Commun.*, Vol. 281, 5664–5670, 2008.
12. Ahmed, S. and Q. A. Naqvi, "Electromagnetic scattering of two or more incident plane waves by a perfect electromagnetic conductor cylinder coated with a metamaterial," *Progress In Electromagnetics Research B*, Vol. 10, 75–90, 2008.
13. Fiaz, M. A., A. Ghaffar, and Q. A. Naqvi, "High frequency expressions for the field in the caustic region of a PEMC cylindrical reflector using Maslov's method," *Journal of Electromagnetic Waves and Applications*, Vol. 22, 358–397, 2008.
14. Fiaz, M. A., A. Ghaffar, and Q. A. Naqvi, "High frequency expressions for the field in the caustic region of a PEMC gregorian system using Maslov's method," *Progress In Electromagnetics Research*, PIER 81, 135–148, 2008.
15. Illahi, A. and Q. A. Naqvi, "Scattering of an arbitrarily oriented dipole field by an intinite and a finite length PEMC circular cylinder," *Central European Journal of Physics*, 2009.
16. Illahi, A., M. Afzaal, and Q. A. Naqvi, "Scattering of dipole field by a perfect electromagnetic conductor cylinder," *Progress In Electromagnetics Research Letters*, Vol. 4, 43–53, 2008.
17. Tang, C. C. H., "Back-scattering from dielectrically coated infinite cylindrical obstacles," Ph.D. Thesis, Harvard University, 1956.

18. Tang, C. C. H., "Backscattering from dielectrically coated infinite cylindrical obstacles," *J. Appl. Phys.*, Vol. 28, 628–633, 1957.
19. Wang, N., "Electromagnetic scattering from a dielectric coated circular cylinder," *IEEE Trans. Antennas Propag.*, Vol. 33, No. 9, 960–963, 1985.
20. Chen, H. C. and D. K. Cheng, "Scattering of electromagnetic waves by an anisotropic plasma-coated conducting cylinder," *IEEE Trans. Antennas Propag.*, Vol. 12, 348–353, 1964.
21. Shen, Z. X., "Electromagnetic scattering by an impedance cylinder coated eccentrically with a chiroplasma cylinder," *IEE Proc. Microw. Antennas Propag.*, Vol. 141, 279–284, Aug. 1994.
22. Shen, Z. and C. Li, "Electromagnetic scattering by a conducting cylinder coated with metamaterials," *Progress In Electromagnetics Research*, PIER 42, 91–105, 2003.
23. Mushref, M. A., "Transverse magnetic scattering of two incident plane waves by a dielectric coated cylindrical reflector," *Central European Journal of Physics*, Vol. 3, No. 2, 229–246, 2005.
24. Mushref, M. A., "Closed solution to electromagnetic scattering of a plane wave by an eccentric cylinder coated with metamaterials," *Opt. Commun.*, Vol. 270, 441–446, 2007.
25. Sun, J., W. Sun, T. Jiang, and Y. Feng, "Directive electromagnetic radiation of a line source scattered by a conducting cylinder coated with left-handed metamaterial," *Microw. Opt. Technol. Lett.*, Vol. 47, 274–279, 2005.
26. Pendry, J. B., A. J. Holden, D. J. Robbins, and W. J. Stewart, "Magnetism from conductors and enhanced nonlinear phenomena," *IEEE Trans. Microw. Theory Tech.*, Vol. 47, No. 11, 1999.
27. Irci, E and V. B. Ertürk, "Achieving transparency and maximizing scattering with metamaterial-coated conducting cylinders," *Physical Review E*, Vol. 76, No. 056603, 2007.
28. Ahmed, S. and Q. A. Naqvi, "Directive EM radiation of a line source in the presence of a coated nihility cylinder," *J. of Electromagn. Waves and Appl.*, Vol. 23, 761–771, 2009.